

See discussions, stats, and author profiles for this publication at: <https://www.researchgate.net/publication/44577211>

On the Molecular Structure and UV/vis Spectroscopic Properties of the Solvatochromic and Thermochromic Pyridinium–N–Phenolate Betaine Dye B30

ARTICLE *in* THE JOURNAL OF PHYSICAL CHEMISTRY A · JUNE 2010

Impact Factor: 2.69 · DOI: 10.1021/jp1009302 · Source: PubMed

CITATIONS

41

READS

46

3 AUTHORS, INCLUDING:



Christian Reichardt

Philipps University of Marburg

195 PUBLICATIONS 5,658 CITATIONS

SEE PROFILE

On the Molecular Structure and UV/vis Spectroscopic Properties of the Solvatochromic and Thermochromic Pyridinium-*N*-Phenolate Betaine Dye B30

Javier Catalán* and Jose Luis Garcia de Paz

Departamento de Química Física Aplicada, Universidad Autónoma de Madrid, 28049 Madrid, Spain

Christian Reichardt

Fachbereich Chemie, Philipps-Universität, Hans-Meerwein-Strasse, 35032 Marburg, Germany

Received: January 31, 2010; Revised Manuscript Received: April 12, 2010

Quantum chemical calculations as well as vis absorption and fluorescence measurements of the pyridinium-*N*-phenolate betaine dye **B30**, dissolved in 1-chlorobutane at temperatures between 343 and 77 K, shed more light on the solvatochromism, thermosolvatochromism, and photophysical behavior of this probe dye, formerly used to establish an empirical scale of solvent polarity, called $E_T(30)$ or E_T^N scale. A new calculated gas-phase $E_T(30)$ value is reported. Complementary to recent work of Kharlanov and Rettig (*J. Phys. Chem. A* **2009**, *113*, 10693–10703), it is shown that fluorescence of **B30** in 1-chlorobutane solution is observable already at temperatures just below the solvent's melting point and not only at 77 K. Analogous to increasing solvent polarity, decreasing solvent temperature leads to a large hypsochromic shift of the vis absorption band of **B30**, dissolved in 1-chlorobutane ($\Delta\lambda = -245$ nm from 797 nm at 343 K to 552 nm at 77 K). This thermosolvatochromism can be easily seen: the solution color changes from greenish yellow (343 K) to magenta–violet (77 K).

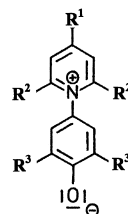
1. Introduction

Solutions of the betaine dye 2,6-diphenyl-4-(2,4,6-triphenylpyridinium-1-yl)phenolate (betaine-30, **B30**; Scheme 1) are solvatochromic, thermochromic, piezochromic, and halochromic. That means that the longest-wavelength intramolecular charge-transfer (CT) vis absorption band of **B30** depends on solvent polarity, solution temperature, external pressure, and on the nature and concentration of added salts.^{1,2} The extraordinary negative solvatochromism of **B30** has been used to establish UV/vis spectroscopically derived empirical parameters of solvent polarity, called $E_T(30)^{3a}$ or E_T^N values.^{3b} $E_T(30)$ values are simply defined as the molar electronic transition energies of **B30**, measured in solvents of different polarity at room temperature (25 °C) and normal pressure (1 bar), according to eq 1

$$E_T(30) \text{ (kcal/mol)} = h \cdot c \cdot \tilde{\nu}_{\max} \cdot N_A = 28\,591/\lambda_{\max} \text{ (nm)} \quad (1)$$

The normalized E_T^N values introduced later on are dimensionless values, using water ($E_T^N = 1.0$) and tetramethylsilane ($E_T^N = 0.00$) as reference solvents.^{3b} Because betaine dye **B30**^{3a} is not soluble in nonpolar solvents such as hydrocarbons and is only sparingly soluble in water, the more lipophilic penta-*t*-butyl-substituted betaine dye **B31**^{3b,g} and the better water-soluble tris-pyridyl-substituted dye **B32**^{3c,g} have been introduced as secondary probe dyes for the determination of $E_T(30)$ values of nonpolar and aqueous media, respectively. All three betaine dyes are (reversibly) protonated at the phenolate oxygen in acidic solvents; then, the solvatochromic vis absorption band disappears. To overcome this difficulty at least partially, the less basic

SCHEME 1: Molecular Structure of the Pyridinium-*N*-phenolate Betaine Dyes B30,^{3a} B31,^{3b,3g} B32,^{3c,3g} and B33^{3d} Used for the Determination of $E_T(30)$ Values As Well As for the Basic Chromophore 4-(Pyridinium-1-yl)phenolate (PyPo)^{3e,10,19c}



	B30	B31	B32	B33	PyPo
R ¹	H ₃ C ₆	4-Me ₃ C-C ₆ H ₄	4-Pyridyl	H ₃ C ₆	H
R ²	H ₃ C ₆	4-Me ₃ C-C ₆ H ₄	H ₃ C ₆	H ₃ C ₆	H
R ³	H ₃ C ₆	4-Me ₃ C-C ₆ H ₄	3-Pyridyl	Cl	H

dichloro-substituted betaine dye **B33**^{3d} and some fluoro- and trifluoromethyl-substituted derivatives of **B30**^{3f} were introduced, which are suitable for measurements in weakly acidic media. Because the E_T values of **B31**–**B33**^{3d,g} correlate linearly with the $E_T(30)$ values of **B30**, $E_T(30)$ values can be calculated from the vis spectra of these secondary standard dyes for solvents, in which **B30** is not soluble.

$E_T(30)$ and E_T^N values are known for a great variety of molecular^{1–3} and ionic solvents.⁴ In addition, they have found many further applications, that is, for the characterization of microheterogeneous solvent systems (e.g., micelles and similar organized media), surfaces (e.g., silica, alumina, cellulose), glasses (e.g., sol ↔ gel systems), solids (e.g., polymers), and for the construction of chemical sensors; see ref 5 for a recent review. The more general term perichromism has been proposed

* To whom correspondence should be addressed. E-mail: javier.catalan@uam.es.

to describe the behavior of **B30** and other solvatochromic dyes in molecular-microscopic surroundings other than solvent spheres.⁶

To rationalize the behavior of **B30** and its sensitivity against even small changes in its molecular-microscopic environment, this class of zwitterionic dyes has been repeatedly and intensively studied.^{1,5,7} Nevertheless, the perichromism of these betaine dyes is far from being well understood. New findings with respect to their solvatochromic,^{8–10} thermochromic,^{11–13} photophysical,^{10,11,13} and structural behavior¹⁰ have been recently reported; some of them will be commented on in this work.

To compare results of theoretical calculations of the vis spectrum of **B30** with experimental values, its gas-phase absorption maximum would be of interest. However, because of the negligible volatility of **B30**, up to now, it was not possible to measure its vis/NIR gas-phase absorption spectrum. Extrapolated and calculated gas-phase absorption maxima of **B30** amount to $\lambda_{\max} = 1043$,^{3b} 1059,^{14a} 1053,^{14b} and 1017 nm,^{14c} leading to a gas-phase $E_T(30)$ value of ca. 27 to 28 kcal/mol. More extreme calculated gas-phase $E_T(30)$ values can be found in refs 14d (19.1 kcal/mol \rightarrow 1496 nm) and 14e (33.5 kcal/mol \rightarrow 853 nm). All of these values are in contrast with the gas-phase $E_T(30)$ value deduced recently by Renge⁸ as a result of an analysis of the absorption behavior of **B30** dissolved in two homogeneous sets of solvents, which were characterized by functions of the solvent's refractive index, n , and relative permittivity, ϵ_r . According to Renge, the excitation of **B30** seems to be connected to a large change in its electronic polarizability from 70 Å³ in the ground to ca. 200 Å³ in the first excited state.⁸ As a consequence, Renge surprisingly proposes by extrapolation a gas-phase $E_T(30)$ value of 40.3 ± 2 kcal/mol ($\lambda_{\max} \approx 709$ nm), which corresponds approximately to the $E_T(30)$ value of methyl acetate (38.9 kcal/mol), a less polar non-HBD solvent.^{1b}

However, during the development of a four-parameter equation for the correlation analysis of solvent effects, including scales for the solvent's dipolarity (SdP),⁹ polarizability (SP),¹⁵ acidity (SA),¹⁶ and basicity (SB),¹⁷ Catalán et al.⁹ came to the conclusion that the $E_T(30)$ scale is not sensitive to the solvent's polarizability and that a gas-phase $E_T(30)$ value of 30.5 ± 0.4 kcal/mol ($\lambda_{\max} \approx 937$ nm) is appropriate, which is in acceptable agreement with the values of 27 to 28 kcal/mol proposed by others.^{3b,14a–c}

Recently, Kharlanov and Rettig¹⁰ have found that the vis absorption maxima of **B30**, dissolved in 1-chlorobutane and ethanol and measured at decreasing solution temperature (at 300, 277, 245, 211, and 180 K), correlate linearly with the temperature-dependent relative permittivity function $f(\epsilon_r) = (\epsilon_r - 1)/(2\epsilon_r + 1)$, demonstrating that its vis absorption data are mainly influenced by the solvent's dipolarity.

Former UV/vis spectroscopic studies of **B30** were mainly centered on the determination of its long-wavelength $\pi \rightarrow \pi^*$ absorption in a great variety of solvents to get $E_T(30)$ values for as many solvents and solvent mixtures as possible. Some recent papers gave now further valuable information about the photophysical behavior of **B30** in solution.^{10,11,13}

An unusual narrowing of the vis absorption band of **B30**, embedded in a poly(vinyl butyral) (PVB) film, was found by Renge¹¹ with increasing temperature: the double value of the half-width at half-maximum of the red side of the **B30** vis absorption band decreases by $\Delta\nu = 130 \pm 20$ cm^{−1} (from 4220 to 4090 cm^{−1}) by increasing the temperature from 14 to 291 K, presumably because of an increasing hydrogen-bond symmetrization in the dye/polymer complex (phenolate–O[−]⋯HO–PVB) on heating. The corresponding $E_T(30)$ value of PVB

as medium amounts to 47.2 (at 10 K) and 45.6 kcal/mol (at 293 K), corresponding to a thermochromic band shift of $\Delta\lambda = 22$ nm for $\Delta T = 283$ K. The $E_T(30)$ value of 45.6 kcal/mol found for the HBD-polymer PVB at 20 °C corresponds well to that of 3-pentanol (45.7 kcal/mol^{1b}), having a molecular structure close to that of PVB.

With respect to the strong solvatochromism of **B30**, its fluorosolvatochromism would be also of interest. Whereas solutions of **B30** do not exhibit any fluorescence at room temperature, it was shown quite recently for the first time that **B30** shows indeed fluorescence at low temperatures.^{10,13} Kharlanov and Rettig¹⁰ demonstrated that solutions of **B30** in 1-chlorobutane and ethanol exhibit fluorescence in both solvents at 77 K, which is absent at room temperature. Yoshida et al.¹³ reported that **B30**, dispersed in thin polymer films (e.g., PVA, PMMA, and PS), shows luminescence at 77 K and even at room temperature.

The molecular structure of **B30** has not yet been studied by X-ray diffraction; however, X-ray structure determinations of a few related betaine dyes (and of some of their salts) are known,^{18,19} that is, 2,6-diphenyl-4-[2,6-diphenyl-4-(4-bromophenyl)pyridinium-1-yl]phenolate,¹⁸ 4-(2,4,6-triphenylpyridinium-1-yl)phenolate,^{19a} and the basic chromophore 4-(pyridinium-1-yl)phenolate (**PyPo**; Scheme 1).^{19c} All betaine dyes are not planar: the interplanar angles between the pyridinium and the phenolate moiety amount to 65,¹⁸ 60,^{19a} and 47°,^{19c} respectively, at least in the crystal lattice. The structural characteristics found are in general coherent with the theoretically calculated values for **B30** in its electronic ground state.^{10,14c,20} Kharlanov and Rettig¹⁰ have calculated the geometry of the ground state of **B30** at HF and DFT levels, establishing a molecular structure of **B30**, which explains why solutions of **B30** do not fluoresce at room temperature but at 77 K.

In this work, the molecular structure of **B30** is calculated for its electronic ground and first excited state to evaluate further the changes in its polarizability and dipolarity on excitation. The knowledge of the structural changes taking place during excitation of **B30** should allow us to understand why solutions of **B30** are not fluorescent at room temperature but at 77 K. Moreover, some calculations have been performed for the more lipophilic secondary standard betaine dye 2,6-(di-*t*-butylphenyl)-4-[2,4,6-tri(4-*t*-butylphenyl)pyridinium-1-yl]phenolate, **B31** (Scheme 1).^{3b}

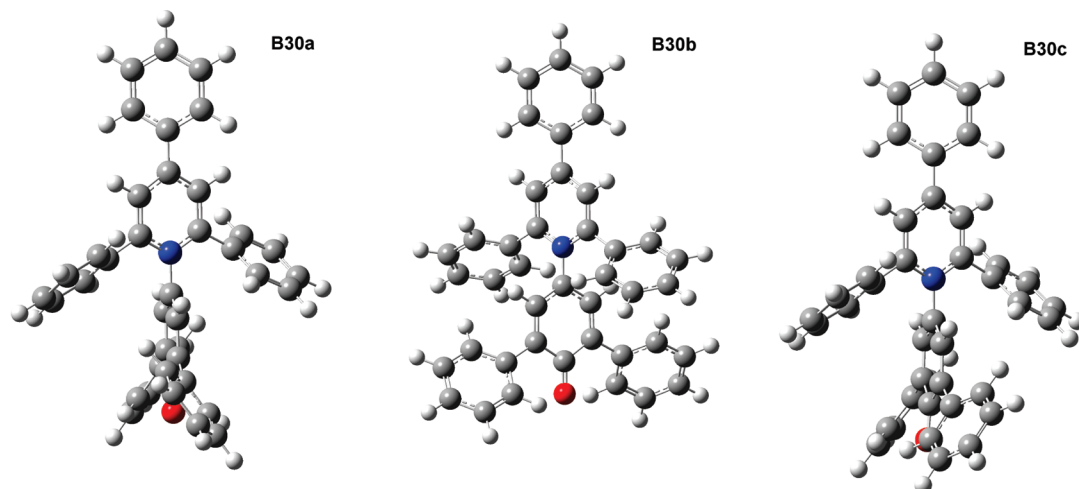
Furthermore, to understand better the sensitivity of **B30**, dissolved in less dipolar non-HBD solvents such as 1-chlorobutane, its vis absorption spectra were measured in the temperature range of 343 to 77 K. This allows us to analyze the nonspecific solvent influence on **B30** and to verify experimentally the sensitivity of the probe dye to the solvent's polarizability. These temperature-dependent vis spectra should also allow us to verify the unexpected results obtained by Renge¹¹ with respect to the vis absorption band narrowing with increasing temperature of **B30** solutions.

2. Experimental and Computational Methods

2.1. Materials. Dilute solutions of **B30** (Sigma-Aldrich), 2-dimethylamino-7-nitrofluorene (**DMANF**; synthesized as described in ref 21), and anthracene (Aldrich; refined by zone-melting) were used. 1-Chlorobutane (Riedel-de Haën) was of spectroscopic quality, free from aromatic impurities.

2.2. Apparatus and Methods. In the range of 77 to 293 K, the temperature of dilute solutions of **B30**, **DMANF**, and anthracene was controlled with an Oxford DN1704 cryostat (purged with dry nitrogen of 99.99% purity), equipped with an

SCHEME 2: S₀ State Optimized Geometries of Three Conformers of B30a–c, Differing Mainly in the Extent of Rotation of Their Peripheral Phenyl Groups



ITC4 controller interfaced to the spectrophotometers. In the temperature range of 293 to 343 K, a Fisons-Haake GH thermostat was used.

The UV/vis absorption spectra were recorded with a Cary-5 spectrophotometer, using Suprasil quartz cells of 1 cm path length. All vis spectroscopic measurements with **B30** were made with freshly prepared solutions to avoid a possible S_N2 alkylation reaction of the phenolate oxygen with 1-chlorobutane.

Corrected fluorescence and fluorescence excitation spectra were obtained with a calibrated Aminco-Bowman AB2 spectrofluorimeter. The sensitivity factors for the emission channel, which include not only those depending on the detector but also those related to the emission monochromator and the optical arrangement (channel emission included), were obtained by using the correction Kit FP-123 from SLM Instruments. This required mounting a standard lamp in a channel at right angles to the emission channel on an OL 245 M spectral irradiance lamp from Optronic Laboratories. The lamp was operated at a constant voltage supplied by an SP-270 power source. Its light output was driven into an integrating sphere with a pinhole leading to the emission channel of the fluorimeter. The conversion factors thus obtained allowed us to convert the measured spectra into absolute spectra, which are independent of the instrument used.

Corrected excitation spectra were directly measured with an AB2 spectrofluorimeter. A small fraction of the light intensity used for excitation was switched to a Hamamatsu S1336-8BQ photodiode by means of a beam splitter. Plotting the photodiode sensitivity as a function of the wavelength allows us to characterize changes in the incident light intensity at each excitation wavelength used. The ratio of the emission intensity at the monitored wavelength to the corresponding excitation intensity at each excitation wavelength was used to construct absolute excitation spectra.

2.3. Calculations. All calculations were performed using the Gaussian 03, revision E.01, package.²² All 4-(4-phenylpyridinium-1-yl)phenolate and **B30** geometries were fully optimized to obtain a true minimum; no imaginary frequencies were found. The ground-state geometry was calculated at the HF and the B3LYP level, using Becke's three-parameter hybrid method²³ with the correlation functional of Lee, Yang, and Parr (LYP)²⁴ with Gaussian 03. The first singlet-excited state of **B30** was computed at the CIS level.²⁵ Although **B30** is a charge-separated

zwitterionic system, the standard 6-31G** basis set²⁶ was used because of its large size and for compatibility with previous studies.

A geometry optimization of the S₁ state of 4-(4-phenylpyridinium-1-yl)phenolate and **B30** was tried at the TDDFT/B3LYP level using the Turbomole 5.7 program;²⁷ however, it could not be performed because of instabilities of this method, as was already found previously by Kharlanov and Rettig.¹⁰ Therefore, for the first singlet-excited state of **B30**, we were restricted to the CIS results.

Analogous calculations have been performed for the penta-*t*-butyl-substituted betaine dye **B31**,^{1b} optimizing its electronic ground state at the HF/6-31G** level.

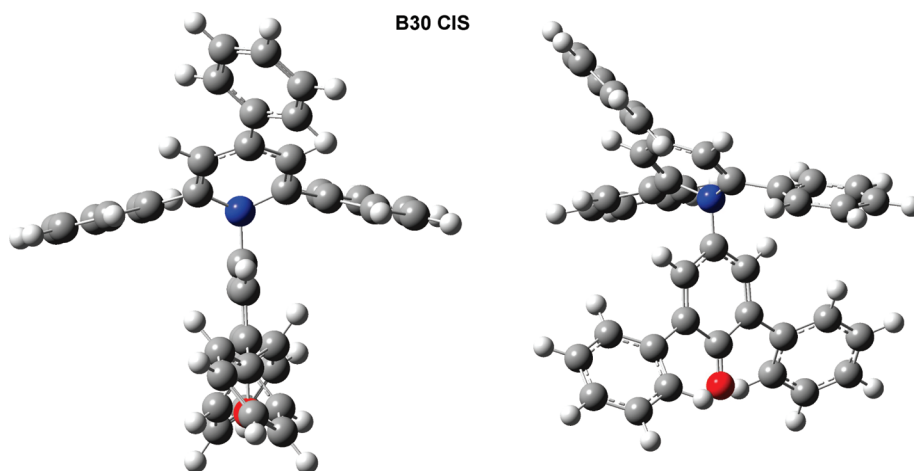
3. Results and Discussion

We will start with an analysis of the theoretical results achieved about the molecular structure and properties of **B30** in its electronic ground (S₀) and first excited (S₁) state. Then, we will analyze the photophysics of **B30**, and, finally, its thermochromic behavior in 1-chlorobutane solution in the temperature range of 77 to 343 K. A new estimate for the gas-phase *E*_T(30) value will be made.

3.1. Molecular Structure of Betaine Dye B30. In its S₀ state we have found three slightly different conformations, **B30a**, **B30b**, and **B30c**, representing true energy minima, with all real vibrational frequencies. (See Scheme 2 and Supporting Information, Table S-1.)

The lowest-energy conformer **B30a** has a dipole moment of 17.9 D and a polarizability of 63.79 Å³. Conformers **B30b** and **B30c** correspond to energy minima, which are slightly higher than that of **B30a**. The interplanar angles between the pyridinium and the phenolate ring amount to ca. −70°, which corresponds satisfactorily to that found by X-ray analysis of a 4-bromo-substituted derivative of **B30** (−65°).¹⁸ Further interplanar angles and the geometrical coordinates of all conformers are collected in the Supporting Information. The geometrical parameters of **B30a** are consistent with those found by Kharlanov and Rettig for its S₀ state.¹⁰

The main structural differences among the three conformers are due to different rotation of the five peripheral phenyl groups. They remain when the three molecular structures are optimized at the B3LYP/6-31G** level (Supporting Information, Table S-1).

SCHEME 3: S_1 State Optimized Geometry of B30 Calculated at the CIS Level

Altogether, our theoretical data show that **B30** in its S_0 state is a highly dipolar and polarizable probe dye, which is in good agreement with the experimental information available for this betaine dye.^{1,5,18,19}

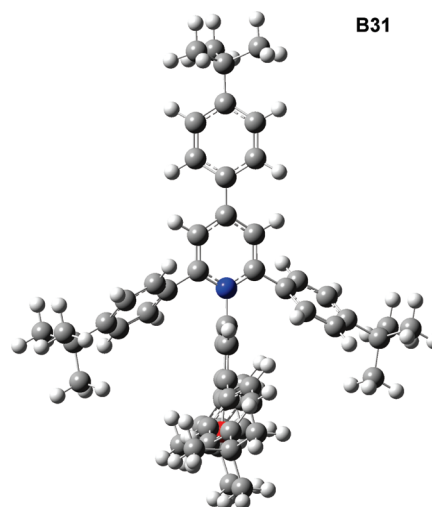
Upon electronic excitation in the S_1 state, which is connected to a CT from the phenolate to the pyridinium moiety, the pyridinium nitrogen atom of **B30** changes dramatically its hybridization to form a strongly pyramidalized nitrogen (angle of 122°), as calculated at the CIS level (Scheme 3 and Supporting Information, Table S-5).

In the S_1 state, the betaine molecule has changed to a much less dipolar structure with a dipole moment of only 2.70 D, but still with a rather high polarizability of 67.05 \AA^3 . According to this, the strong negative solvatochromism of **B30** is mainly caused by the large decrease in the dipole moment during the $\pi \rightarrow \pi^*$ transition (with intramolecular CT character), whereas the negligible change in polarizability on excitation makes **B30** practically insensitive to changes in the solvent's polarizability.

These changes in the molecular structure of **B30** on excitation are mainly determined by the five peripheral phenyl groups attached to the basic betaine chromophore. When a betaine dye without four of these five phenyl groups is studied (i.e., 4-(4-phenylpyridinium-1-yl)phenolate), the nitrogen atom is only slightly pyramidalized (angle of 172°). We have checked this behavior by optimizing the molecular geometry of **B30** and 4-(4-phenylpyridinium-1-yl)phenolate from both starting points, one with and another without a pyramidalized nitrogen atom. The CIS method applied predicts a pyramidalized nitrogen (near sp^3) for **B30** but a nitrogen near sp^2 for the less-substituted 4-(4-phenylpyridinium-1-yl)phenolate, which is very similar to the molecular structure obtained by Kharlanov and Rettig¹⁰ for the nonsubstituted basic betaine dye **PyPo** (Scheme 1).¹⁰

It should be again emphasized that the calculated electronic polarization of **B30** in its ground and first excited states is nearly the same in both states. This means that the long-wavelength $\pi \rightarrow \pi^*$ absorption of **B30** is practically not sensitive to changes in the polarizability of solvents in which it is dissolved. This is a theoretical proof of our former prediction that $E_T(30)$ parameters are practically insensitive to the solvent's polarizability.⁹

The conformation of lowest energy calculated for the more lipophilic penta-*t*-butyl-substituted betaine dye **B31** corresponds to a zwitterionic molecule with a dipole moment of 17.7 D, a polarizability of 90.48 \AA^3 , and an interplanar pyridinium/phenolate angle of -70.1° (Scheme 4 and Supporting Information, Tables S-1 and S-6).

SCHEME 4: S_0 State Optimized Geometry of the Penta-*t*-butyl-substituted Betaine Dye **B31**^{3b,3g}

If one compares the calculated molecular structures of **B30a–c** and **B31**, it can be stated that the introduction of five *t*-butyl groups to the five peripheral phenyl groups of **B30** has no significant influence on the conformational structure of **B31**. The calculated ground-state dipole moments of **B30a–c** and **B31** are practically the same. According to the higher molar mass and size of **B31**, only its polarizability is, as expected, with ca. 90 \AA^3 somewhat larger than that of **B30a–c** (ca. 64 \AA^3). This means that the photophysical results observed for the standard betaine dye **B30** are also applicable to **B31**, and its use as secondary standard dye for the determination of $E_T(30)$ values of nonpolar solvents is justified.

3.2. Photophysical Consequences of Changes in the Molecular Structure during the $S_0 \rightarrow S_1$ Excitation of Betaine Dye B30. Kharlanov and Rettig¹⁰ were not able to optimize the molecular structure of **B30** in its first excited state, but from their model study of the reduced basic chromophore 4-(pyridinium-1-yl)phenolate (**PyPo**; Scheme 1), they propose for the geometry of the S_1 state of **B30** with minimum energy a structure in which pyridinium and phenolate ring are orthogonal to each other, thus representing a molecule of biradical nature, with an unpaired electron at each of the two orthogonal rings. In other words, the Franck–Condon (FC) excited state of **B30** relaxes to a twisted biradical structure, which does not fluoresce because of an easy radiationless deactivation at room temperature.

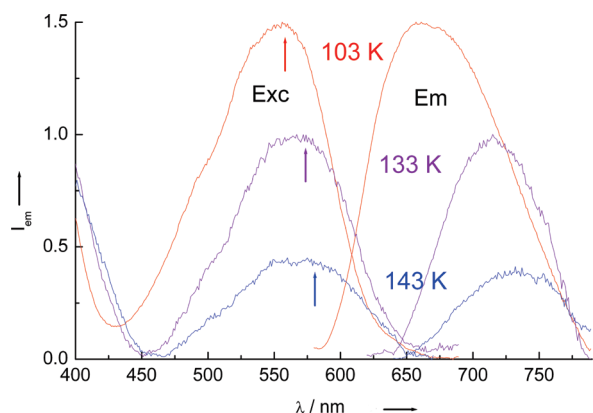


Figure 1. Excitation spectra (monitored at 750 nm) and emission spectra (excitation wavelength 565 nm) of a **B30** solution in 1-chlorobutane (in the maxima, absorbance = 0.1 at room temperature) measured at 103 (red), 133 (violet), and 143 K (blue). The arrows indicate the position of the corresponding maxima of the long-wavelength vis absorption band of the **B30** solutions.

The transformation of the molecular structure of **B30** after excitation as proposed by Kharlanov and Rettig¹⁰ corresponds to a rotation along the long axis of the dye molecule, without drastic deformation of the solvent cage surrounding the dye solute. This negligible change of the solvent cavity during excitation is possibly an explanation for the observation that fluorescence of dissolved **B30** could be detected only at very low temperatures (77 K).

If, however, the structural change of the excited **B30** molecule is as drastic as described in Scheme 3, with strong pyramidalization of the nitrogen atom, then it should not be necessary to decrease the solution temperature to such an extent to get fluorescence. Already, temperatures somewhat below the solvent's melting point should be sufficient to block the solute's structural change, with preservation of the FC state, from which fluorescence is only possible.

In Figure 1, the excitation and emission spectra of **B30** dissolved in 1-chlorobutane measured at three temperatures (143, 133, and 103 K), which are below the solvent's melting point ($T_{mp} = 150$ K), are shown.

The observation that fluorescence already occurs at higher temperatures than 77 K can be best explained as follows: in contrast with the normal behavior of chromophores, the electronic excitation of **B30** to the FC excited state, which is fluorescent, is followed by a geometrical relaxation to the *N*-pyramidalized S_1 state of minimum energy, which does not fluoresce. That is, the pyramidalization at the pyridinium nitrogen occurs after excitation to the FC state, demanding a more drastic rearrangement of the solvent cavity surrounding the **B30** solute, in contrast with the proposal made by Kharlanov and Rettig,¹⁰ which includes only a less demanding rotational relaxation to an orthogonal arrangement of the pyridinium and phenolate ring.

Both proposals have in common that the FC state and the relaxed S_1 state of **B30** are separated by a small barrier dependent on solvent/solute interactions, best described by the solvent's viscosity, as schematically shown in Figure 2. This temperature-dependent barrier determines at which solution temperature (above or below the solvent's melting point) fluorescence of **B30** can be seen or not.

Figure 3 shows the vis absorption spectrum of **B30** dissolved in 1-chlorobutane measured at solution temperatures between 343 and 77 K (with intervals of 10 K). The vis spectrum is of good quality and does not collapse at 180 K with another intense

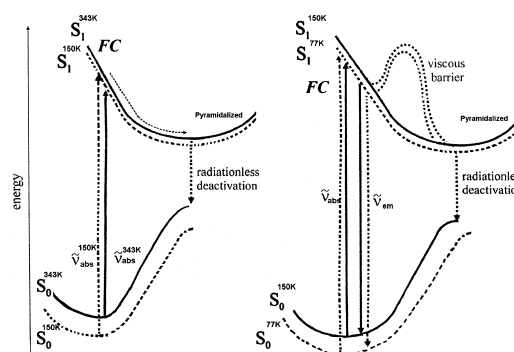


Figure 2. Behavior of **B30**, dissolved in 1-chlorobutane, at various solution temperatures. Left-hand side: behavior of **B30** solutions at temperatures above the melting point of 1-chlorobutane (155 K), which are nonfluorescent because of *N*-pyramidalization of the betaine chromophore after excitation to the FC state. Right-hand side: behavior of **B30** solutions at temperatures below the solvent's melting point, which are fluorescent because the solid solvent does not allow the *N*-pyramidalization of **B30** after excitation to the FC state.

band at ca. 440 nm, as reported by Kharlanov and Rettig (see Figure 2b in ref 10). Table 1 collects all vis absorption maxima of **B30** measured in 1-chlorobutane in the temperature range of 77 to 343 K with intervals of 10 K.

Decreasing the solution temperature by $\Delta T = 266$ K leads to a hypsochromic shift of the vis absorption band of **B30** by $\Delta\tilde{\nu} = 5578$ cm^{-1} ($\Delta\lambda = -245$ nm), which corresponds to an increase in the $E_T(30)$ value for 1-chlorobutane by $\Delta E_T(30) = 16$ kcal/mol from 35.9 (343 K) to 51.8 kcal/mol (77 K). The corresponding thermochromic color change from greenish-yellow (343 K) to magenta-violet (77 K) can easily be seen with the naked eye, which confirms the unusual large thermosolvatochromism found for this type of betaine dyes also in many other media.^{1a,10-13}

The temperature-dependent bandwidths of the vis absorption band of **B30**, measured in 1-chlorobutane in the temperature range of 343 to 77 K, are shown in Figure 4. As can be seen, the bandwidths do not follow the behavior reported by Renge¹¹ for **B30** embedded in a polymeric PVB film, showing a slight steady decrease with increasing temperature from 14 to 291 K. According to Figure 4, three different regions can be recognized: in solid 1-chlorobutane (77 to 133 K), the bandwidth remains practically constant; near the solvent's melting point (between 143 and 183 K), the bandwidth increases; and at higher temperatures (193 to 343 K), the bandwidth decreases significantly by ~ 600 cm^{-1} . At present, we have no simple explanation for this complex behavior.

The behavior of 1-chlorobutane as solvent was also tested by means of the UV/vis absorption spectra of the spectroscopic probes 2-dimethylamino-7-nitrofluorene (**DMANF**) (Figure 5) and anthracene (Figure 6) measured in the same temperature range as that for **B30**. (See Table 1.)

Following the procedure described in ref 9, the UV/vis absorption maxima of **DMANF** and anthracene allow an evaluation of the corresponding parameters describing the solvent dipolarity (SdP) and solvent polarizability (SP) of 1-chlorobutane for a large temperature range ($\Delta T = 266$ K), which are also collected in Table 1. First, it must be proven that the procedures used to evaluate these parameters at room temperature are equally appropriate for such a large temperature range.

In the literature, relative permittivities, ϵ_r , for 1-chlorobutane were found for 14 temperatures between 343 and 183 K,²⁸⁻³⁰ which allow us to calculate the following empirical linear

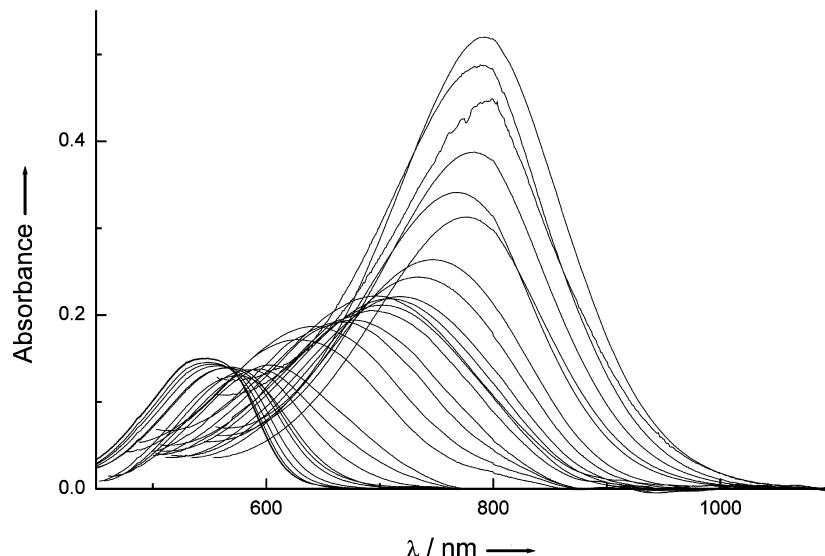


Figure 3. Long-wavelength vis absorption band of **B30**, dissolved in 1-chlorobutane measured at solution temperatures between 343 and 77 K.

TABLE 1: Experimental Wavenumbers for the Peak Maxima of the Long-Wavelength Absorption band of B30 and DMANF As Well As the 0-0 Component of the First Absorption Band of Anthracene Measured in 1-Chlorobutane at Various Temperatures (from +70 to −196 °C) and the Corresponding $E_T(30)$, SdP , and SP Values (See Text)

T/K	$\tilde{\nu}_{\max}/\text{cm}^{-1}$ (B30)	$\tilde{\nu}_{\max}/\text{cm}^{-1}$ (DMANF)	$\tilde{\nu}_{0-0}/\text{cm}^{-1}$ (anthracene)	$E_T(30)/(\text{kcal/mol})$	SdP	SP
343	12 547	24 386	26 605	35.9	0.399	0.654
333	12 635	24 314	26 593	36.1	0.422	0.661
323	12 658	24 223	26 582	36.2	0.457	0.668
313	12 786	24 126	26 571	36.6	0.496	0.675
303	12 886	24 047	26 558	36.8	0.521	0.683
293	13 025	23 950	26 547	37.2	0.560	0.690
283	13 229	23 860	26 533	37.8	0.589	0.699
273	13 477	23 785	26 527	38.5	0.623	0.703
263	13 767	23 713	26 518	39.4	0.653	0.708
253	13 956	23 624	26 509	39.9	0.690	0.714
243	14 095	23 559	26 496	40.3	0.706	0.722
233	14 190	23 471	26 484	40.6	0.739	0.729
223	14 272	23 383	26 476	40.8	0.778	0.734
213	14 613	23 300	26 467	41.8	0.812	0.740
203	14 886	23 202	26 452	42.6	0.845	0.749
193	15 443	23 120	26 440	44.2	0.875	0.756
183	15 778	23 025	26 430	45.1	0.913	0.763
173	16 413	22 931	26 420	46.9	0.953	0.769
163	16 583	22 865	26 410	47.4	0.976	0.775
153	16 925	22 769	26 399	48.4	1.014	0.782
143	17 222	22 685	26 388	49.2	1.045	0.789
133	17 418	22 596	26 373	49.8	1.073	0.798
123	17 531	22 423	26 363	50.1	1.162	0.804
113	17 791	22 337	26 354	50.9	1.197	0.810
103	17 919	22 271	26 344	51.2	1.220	0.816
93	18 061	22 206	26 338	51.6	1.248	0.820
83	18 125	22 139	26 331	51.8	1.278	0.824
77	18 125	22 107	26 329	51.8	1.294	0.825

$$\Delta T = 266 \text{ K} \quad \Delta \tilde{\nu} = 5578 \text{ cm}^{-1} \quad \Delta \tilde{\nu} = -2279 \text{ cm}^{-1} \quad \Delta \tilde{\nu} = -276 \text{ cm}^{-1} \quad \Delta E_T(30) = 16 \text{ kcal/mol} \quad \Delta SdP = 0.895 \quad \Delta SP = 0.171$$

relationship between the permittivity function $f(\epsilon_r)$ and the absolute temperature of 1-chlorobutane

$$f(\epsilon_r) = (\epsilon_r - 1)/(2\epsilon_r + 1) = -0.00034 \cdot T + 0.5044$$

(with $n = 14$; $r = 0.9991$; $sd = 0.0007$)

(2)

When eq 2 is used to calculate $f(\epsilon_r)$ and SdP values for other temperatures than those already known, and they were used for

checking the existing experimental SdP values, and eventually, all SdP values are plotted against $f(\epsilon_r)$, a good linear correlation is found as shown in Figure 7. This means that the SdP values of 1-chlorobutane describe reliable its dipolarity within a large temperature range.

Assuming that the molar refraction, R , of 1-chlorobutane does not change its value with temperature, the Lorentz–Lorenz equation can be used to evaluate the polarizability function, $f(n^2)$, at a given temperature, using existing data for the density of 1-chlorobutane^{28,29} for this temperature by means of eq 3 (M_r

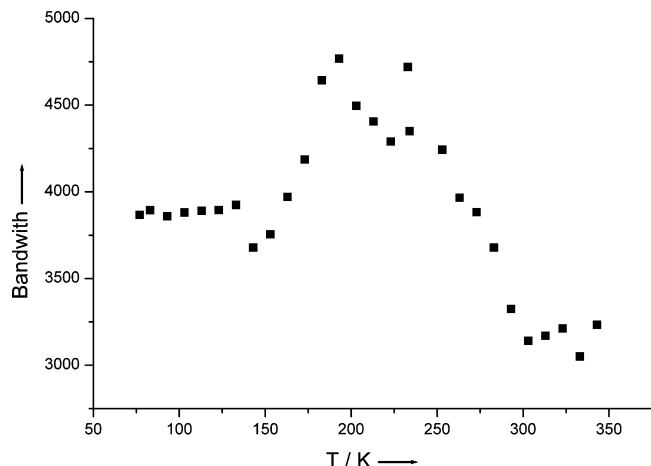


Figure 4. Behavior of the bandwidths of the long-wavelength vis absorption band of **B30** dissolved in 1-chlorobutane at various temperatures.

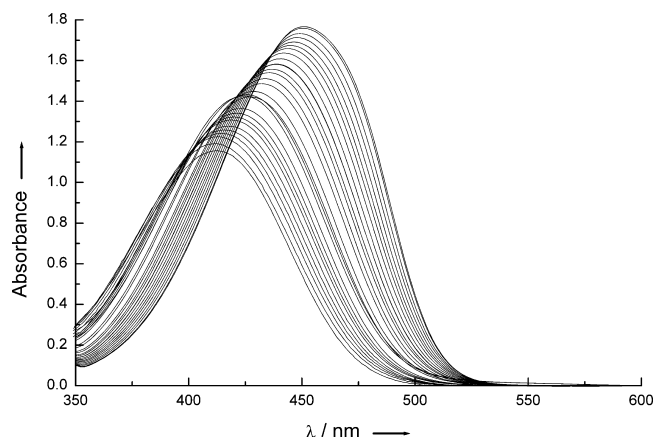


Figure 5. Long-wavelength vis absorption band of 2-dimethylamino-7-nitrofluorene (**DMANF**) dissolved in 1-chlorobutane measured at solution temperatures between 343 and 77 K.

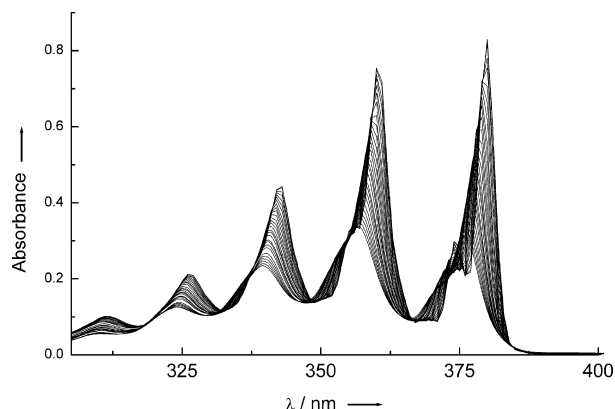


Figure 6. Long-wavelength UV absorption band of anthracene dissolved in 1-chlorobutane measured at solution temperatures between 343 and 77 K.

= relative molar mass; ρ = mass density), with an R previously calculated using values of n and ρ for the temperature given.

$$f(n^2) = (n^2 - 1)/(n^2 + 2) = R/M_r \cdot \rho \quad (3)$$

Plotting the polarizability function $f(n^2)$, evaluated with the density data given in refs 28 and 29 against the solvent's

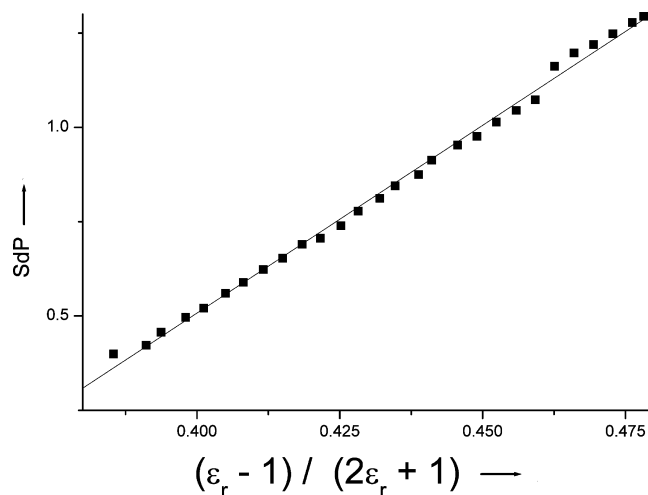


Figure 7. Linear correlation between the SdP parameter and the relative permittivity function $f(\epsilon_r) = (\epsilon_r - 1)/(2\epsilon_r + 1)$ of 1-chlorobutane between 343 and 77 K. (See the text.)

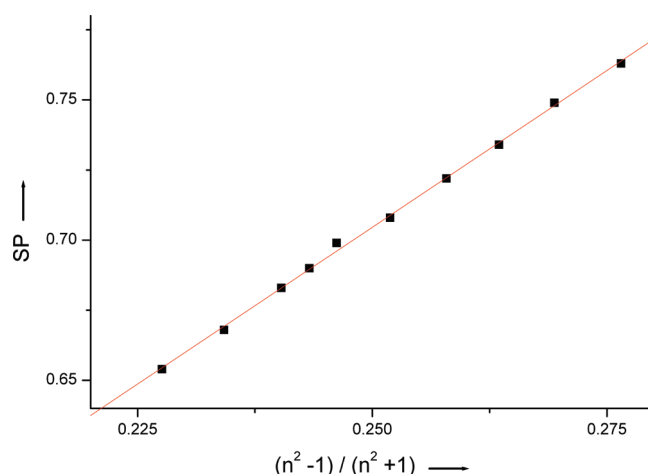


Figure 8. Linear correlation between the SP parameter and the electronic polarizability function $f(n^2) = (n^2 - 1)/(n^2 + 1)$ of 1-chlorobutane between 343 and 77 K. (See the text.)

polarizability parameter, SP , an excellent linear correlation results, as shown in Figure 8.

Because both solvent parameters SdP and SP describe the dipolarity and polarizability of 1-chlorobutane obviously appropriate for the large temperature range applied, we have in hand a good tool to analyze now the behavior of **B30**, dissolved in 1-chlorobutane, in this wide temperature range.

1-Chlorobutane is a less dipolar ($\mu = 1.90$ D at 20 °C in CCl_4 ; $\epsilon_r = 7.39$ at 20 °C³¹) non-HBD solvent and will interact with dissolved **B30** by dipolarity and polarizability interaction forces only. Therefore, the dependence of the $E_T(30)$ value of 1-chlorobutane on the parameters for its dipolarity, SdP , and polarizability, SP , has been studied, resulting in the correlation eqs 4–6 for $n = 28$ data pairs

$$E_T(30) \text{ (kcal/mol)} = (10.87 \pm 8.69) \cdot SdP + (49.52 \pm 44.92) \cdot SP - (2.50 \pm 26.19) \quad (4)$$

$$E_T(30) \text{ (kcal/mol)} = (105.64 \pm 3.19) \cdot SP - (35.13 \pm 2.38) \quad (5)$$

$$E_T(30) \text{ (kcal/mol)} = (20.43 \pm 0.61) \cdot SdP + (26.39 \pm 0.54) \quad (6)$$

All three correlations are very good with correlation coefficients of $r = 0.9889$, 0.9884 , and 0.9884 , respectively. However, eqs 4 and 5 have no physical meaning for the following reasons: (a) both equations predict a negative $E_T(30)$ value for the gas phase (for which $SdP = SP = 0$) because the intercepts of the two correlation equations have a negative sign; (b) in both equations the regression coefficient of the parameter measuring the solvent's polarizability, SP , is positive. This would mean that the vis absorption band of **B30** would be strongly shifted hypsochromically with decreasing temperature, which is only possible when the electronic polarizability of **B30** in the S_1 excited state is much smaller than that in the S_0 ground state. However, as expected, eq 6 is physically coherent with the existing experimental evidence because it is accepted that **B30** possesses a large dipole moment in the S_0 ground state and a rather small one in its S_1 excited state. As consequence, the values of $E_T(30)$ increase with increasing dipolarity of 1-chlorobutane at decreasing solution temperatures. In addition, the intercept of eq 6, representing the gas-phase $E_T(30)$ value, is with 26.39 ± 0.54 kcal/mol (corresponding to $\lambda_{\max} \approx 1083$ nm) in good agreement with the gas-phase $E_T(30)$ values of 27 to 28 kcal/mol found earlier by extrapolation^{3b} or calculations.^{14a-c} (See the Introduction.)

Obviously, the solvatochromic probe dye **B30**, dissolved in 1-chlorobutane, measures only the change in dipolarity of 1-chlorobutane while changing the temperature; it is not sensitive to changes in the solvent's polarizability. In conclusion, dissolved **B30** is an excellent probe for measuring the dipolarity of neutral non-HBD solvents with changing solution temperature.

4. Conclusions

The outstanding sensitivity of the negatively solvatochromic and thermochromic pyridinium-*N*-phenolate betaine dye **B30** against small changes in its molecular-microscopic environment is caused by differential solvation of its electronic S_0 ground and its S_1 excited state. Increasing solvation capability (solvent polarity) of the solvents used leads to a better stabilization of the highly dipolar ground state relative to the much less dipolar excited state, with a large hypsochromic band shift of the long-wavelength $\pi-\pi^*$ vis absorption band as consequence. Increasing differential solvation between the ground and excited state of **B30**, dissolved in one solvent only (e.g., 1-chlorobutane), with decreasing solution temperature leads also to a hypsochromic band shift, representing a new type of thermochromism called thermosolvatochromism.^{1,12}

This is in agreement with quantum chemical calculations, which exhibit for the S_0 ground state of **B30** three highly dipolar and polarizable conformers, differing mainly in the extent of rotation of the five peripheral phenyl groups (Scheme 2 and Supporting Information, Table S-1). The FC S_1 excited state of **B30**, the result of a $\pi \rightarrow \pi^*$ transition with pronounced intramolecular CT character, relaxes to a less dipolar, but equally polarizable excited state with a highly pyramidalized pyridinium nitrogen (Scheme 3). The calculated, nearly equal electronic polarizability of **B30** in its ground and first excited state confirms previous predictions about the insensitivity of the $E_T(30)$ parameters against changes of the solvent's polarizability.⁹

Decisive for the appearance of fluorescence of dissolved **B30** at low temperatures is the solvent-dependent viscous barrier between the fluorescent FC S_1 excited state and the final nonfluorescent relaxed S_1 excited state, from which a radiationless deactivation takes place (Figure 2). According to our calculations, the relaxed S_1 excited state of **B30** is with its highly pyramidalized nitrogen sterically much more demanding than

the orthogonal pyridinium/phenolate arrangement proposed by Kharlanov and Rettig.¹⁰ Therefore, the transition from the FC to the relaxed S_1 excited state of **B30** causes a larger change of the surrounding solvent cavity. Therefore, this transition can be made more difficult already at higher solution temperatures just below the melting point of the solvent 1-chlorobutane (150 K). This explains the observation that fluorescence of **B30** solutions in 1-chlorobutane have been found already at temperatures of 143, 133, and 103 K. This photophysical behavior can be considered as a kind of singular behavior, but we hesitate to call it an *anti* Kasha behavior.

A gas-phase $E_T(30)$ value of ca. 26.4 kcal/mol ($E_T^N \approx -0.133$) has been determined by calculations using the SP and SdP parameters introduced by Catalán;⁹ this value is in excellent agreement with that of 27 to 28 kcal/mol found in former work.^{3b,14a-c}

Acknowledgment. We are greatly indebted to the *Centro de Computacion Cientifica* (CCC) of the *Universidad Autónoma de Madrid*, Spain, for access to their computing facilities and the available computer time.

Supporting Information Available: Results of quantum chemical calculations and geometrical coordinates. This material is available free of charge via the Internet at <http://pubs.acs.org>.

References and Notes

- (1) (a) Reichardt, C. *Chem. Soc. Rev.* **1992**, *21*, 147–153. (b) Reichardt, C. *Chem. Rev.* **1994**, *94*, 2319–2358. (c) Reichardt, C. *Org. Process Res. Dev.* **2007**, *11*, 105–113.
- (2) Reichardt, C. *Solvents and Solvent Effects in Organic Chemistry*, 3rd ed.; Wiley-VCH: Weinheim, Germany, 2003; Chapters 6.2 and 7.4.
- (3) (a) Dimroth, K.; Reichardt, C.; Siepmann, T.; Bohlmann, F. *Justus Liebigs Ann. Chem.* **1963**, 661, 1–37. $E_T(30)$ values in kilocalories per mole (range ca. 31–63 kcal/mol). In this first paper, the standard betaine dye **B30** had by chance the formula number **30**. (b) Reichardt, C.; Harbusch-Görnert, E. *Liebigs Ann. Chem.* **1983**, 721–743. Introduction of normalized dimensionless E_T^N values (range 0–1). (c) Reichardt, C.; Che, D.; Heckenkemper, G.; Schäfer, G. *Eur. J. Org. Chem.* **2001**, 2343–2361. (d) Kessler, M. A.; Wolfbeis, O. S. *Chem. Phys. Lipids* **1989**, *50*, 51–56. Introduction of $E_T(33)$ values. (e) Gonzáles, D.; Neilands, O.; Rezende, M. C. *J. Chem. Soc., Perkin Trans. I* **1999**, 713–717. See also ref 19c. (f) Reichardt, C.; Eschner, M.; Schäfer, G. *J. Phys. Org. Chem.* **2001**, *14*, 737–751. (g) For consistency with $E_T(30)$, it is now recommended to call E_T values of the secondary standard betaine dyes **B31** and **B32** $E_T(31)$ and $E_T(32)$ values, respectively; for $E_T(33)$, see ref 3d.
- (4) Reichardt, C. *Green Chem.* **2005**, *7*, 339–351.
- (5) Reichardt, C. *Pure Appl. Chem.* **2008**, *80*, 1415–1432.
- (6) Kosower, E. M. Tel Aviv University, Tel Aviv, Israel. Private communication to C.R., 1994. See also ref 1b.
- (7) (a) Koppel, I. A.; Palm, V. A. The Influence of the Solvent on Organic Reactivity. In *Advances in Linear Free Energy Relationships*; Chapman, N. B., Shorter, J., Eds.; Plenum Press: New York, 1972; Chapter 5, p 203. (b) Chastrette, M.; Carretto, J. *Tetrahedron* **1982**, *38*, 1615–1618. (c) Bekárek, V.; Juřina, J. *Collect. Czech. Chem. Commun.* **1982**, *47*, 1060–1068. (d) Makitra, R. G.; Pirig, Ya. N.; Kivilyuk, R. B. *Zh. Obshch. Khim.* **1990**, *60*, 2209–2215; *Chem. Abstr.* **1991**, *114*, 24650e. (e) Marcus, Y. *Chem. Soc. Rev.* **1993**, *22*, 409–416. (f) Catalán, J. Solvent Effects Based on Pure Solvent Scales. In *Handbook of Solvents*; Wypych, G., Ed.; ChemTec Publishing: Toronto, 2001; Chapter 10.3, p 583. (g) Abboud, J.-L. M.; Notario, R. *Pure Appl. Chem.* **1999**, *71*, 645–718. (h) Katritzky, A. R.; Fara, D. C.; Yang, H.; Tamm, K.; Tamm, T.; Karelson, M. *Chem. Rev.* **2004**, *104*, 175–198.
- (8) Renge, I. *Chem. Phys. Lett.* **2008**, *459*, 124–128.
- (9) Catalán, J. *J. Phys. Chem. B* **2009**, *113*, 5951–5960.
- (10) Kharlanov, V.; Rettig, W. *J. Phys. Chem. A* **2009**, *113*, 10693–10703.
- (11) Renge, I. *J. Lumin.* **2009**, *129*, 469–473.
- (12) (a) Dimroth, K.; Reichardt, C.; Schweig, A. *Justus Liebigs Ann. Chem.* **1963**, 669, 95–105. (b) Bubltz, G. U.; Boxer, S. G. *J. Am. Chem. Soc.* **1998**, *120*, 3988–3992. (c) Zhao, X.; Burt, J. A.; Knorr, F. J.; McHale, J. L. *J. Phys. Chem. A* **2001**, *105*, 11110–11117. (d) Martins, C. T.; Lima, M. S.; Bastos, E. L.; El Seoud, O. A. *Eur. J. Org. Chem.* **2008**, 1165–1180. (e) Martins, C. T.; Sato, B. M.; El Seoud, O. A. *J. Phys. Chem. B* **2008**, *112*, 8330–8339.

- (13) Nishiyama, S.; Aikawa, S.; Tajima, M.; Yoshida, Y. *Mol. Cryst. Liq. Cryst.* **2007**, *462*, 257–265. *ibid.* **2008**, *492*, 130–138.
- (14) (a) Jano, I. *J. Chim. Phys. Phys.-Chim. Biol.* **1992**, *89*, 1951–1971. (b) Streck, C.; Richert, R. *Ber. Bunsen-Ges.* **1994**, *98*, 619–625. (c) Caricato, M.; Mennucci, B.; Tomasi, J. *Mol. Phys.* **2006**, *104*, 875–887. (d) Masternak, A.; Wenska, G.; Milecki, J.; Skalski, B.; Franzen, St. J. *Phys. Chem. A* **2005**, *109*, 759–766 (supporting information). (e) Fabian, J. *Dyes Pigm.* **2009**, *84*, 36–53 (Figure 3: dye 95).
- (15) Catalán, J.; Hopf, H. *Eur. J. Org. Chem.* **2004**, 4694–4702.
- (16) (a) Catalán, J.; Díaz, C. *Liebigs Ann./Recl.* **1997**, 1941–1949. (b) Catalán, J.; Díaz, C. *Eur. J. Org. Chem.* **1999**, 885–891.
- (17) Catalán, J.; Díaz, C.; López, V.; Pérez, P.; De Paz, J.-L. G.; Rodríguez, J. G. *Liebigs Ann.* **1996**, 1785–1794.
- (18) Allmann, R. Z. *Kristallogr.* **1969**, *128*, 115–132.
- (19) (a) Stadnicka, K.; Milart, P.; Olech, A.; Olszewski, P. K. *J. Mol. Struct.* **2002**, *604*, 9–18. (b) Wojtas, L.; Milart, P.; Stadnicka, K. *J. Mol. Struct.* **2006**, *782*, 157–164. (c) Wojtas, L.; Pawlica, D.; Stadnicka, K. *J. Mol. Struct.* **2006**, *785*, 14–20.
- (20) (a) De Alencastro, R. B.; Da Motta Neto, J. D.; Zerner, M. C. *Int. J. Quantum Chem.* **1994**, *28*, 361–377. (b) Lipiński, J.; Bartkowiak, W. *J. Phys. Chem. A* **1997**, *101*, 2159–2165. (c) Bartkowiak, W.; Lipiński, J. *J. Phys. Chem. A* **1998**, *102*, 5236–5240. (d) Mente, S. R.; Maroncelli, M. *J. Phys. Chem. B* **1999**, *103*, 7704–7719. (e) Lobaugh, J.; Rosky, P. J. *J. Phys. Chem. A* **1999**, *103*, 9432–9447. *ibid.* **2000**, *104*, 899–907. (f) Hogiu, S.; Dreyer, J.; Pfeiffer, M.; Brzezinka, K.-W.; Werncke, W. *J. Raman Spectrosc.* **2000**, *31*, 797–803. (g) Domínguez, M.; Rezende, M. C. *J. Phys. Org. Chem.* **2010**, *23*, 156–170.
- (21) Catalán, J.; López, V.; Pérez, P.; Martín-Villamil, R.; Rodríguez, J. G. *Liebigs Ann.* **1995**, 241–252.
- (22) Frisch, M. J.; Trucks, G. W.; Schlegel, H. B.; Scuseria, G. E.; Robb, M. A.; Cheeseman, J. R.; Montgomery, J. A., Jr.; Vreven, T.; Kudin, K. N.; Burant, J. C.; Millam, J. M.; Iyengar, S. S.; Tomasi, J.; Barone, V.; Mennucci, B.; Cossi, M.; Scalmani, G.; Rega, N.; Petersson, G. A.; Nakatsuji, H.; Hada, M.; Ehara, M.; Toyota, K.; Fukuda, R.; Hasegawa, J.; Ishida, M.; Nakajima, T.; Honda, Y.; Kitao, O.; Nakai, H.; Klene, M.; Li, X.; Knox, J. E.; Hratchian, H. P.; Cross, J. B.; Bakken, V.; Adamo, C.; Jaramillo, J.; Gomperts, R.; Stratmann, R. E.; Yazyev, O.; Austin, A. J.; Cammi, R.; Pomelli, C.; Ochterski, J. W.; Ayala, P. Y.; Morokuma, K.; Voth, K. A.; Salvador, P.; Dannenberg, J. J.; Zakrzewski, V. G.; Dapprich, S.; Daniels, A. D.; Strain, M. C.; Farkas, O.; Malick, D. K.; Rabuck, A. D.; Raghavachari, K.; Foresman, J. B.; Ortiz, J. V.; Cui, Q.; Baboul, A. G.; Clifford, S.; Cioslowski, J.; Stefanov, B. B.; Liu, G.; Liashenko, A.; Piskorz, P.; Komaromi, I.; Martin, R. L.; Fox, D. J.; Keith, T.; Al-Laham, M. A.; Peng, C. Y.; Nanayakkara, A.; Challacombe, M.; Gill, P. M. W.; Johnson, B.; Chen, W.; Wong, M. W.; Gonzalez, C.; Pople, J. A. *Gaussian 03*, revision E.01; Gaussian, Inc.: Wallingford, CT, 2004.
- (23) (a) Becke, A. D. *Phys. Rev. A* **1988**, *38*, 3098–3100. (b) Becke, A. D. *J. Chem. Phys.* **1993**, *98*, 5648–5652.
- (24) Lee, C.; Yang, W.; Parr, R. G. *Phys. Rev. B* **1988**, *37*, 785–789.
- (25) Foresman, J. B.; Head-Gordon, M.; Pople, J. A.; Frisch, M. J. *J. Phys. Chem.* **1992**, *96*, 135–149.
- (26) The 6-31G** basis set and the HF method are described in: Hehre, W. J.; Radom, L.; Schleyer, P. v. R.; Pople, J. A. *Ab Initio Molecular Orbital Theory*; Wiley: New York, 1986.
- (27) (a) Ahlrichs, R.; Bär, M.; Häser, M.; Horn, H.; Kölmel, Ch. *Chem. Phys. Lett.* **1989**, *162*, 165–169. (b) Ahlrichs, R.; Bär, M.; Baron, H.-P.; Bauernschmitt, R.; Böcker, S.; Deglmann, P.; Ehrig, M.; Eichkorn, K.; Elliott, S.; Furche, F.; Haase, F.; Häser, M.; Horn, H.; Hättig, Ch.; Huber, Ch.; Huniar, U.; Kattank, M.; Köhn, A.; Kölmel, Ch.; Kollwitz, M.; May, K.; Ochsenfeld, Ch.; Öhm, H.; Schäfer, A.; Schneider, U.; Sierka, M.; Treutler, O.; Unterreiner, B.; von Arnim, M.; Weigend, F.; Weis, P.; Weiss, H. *TURBOMOLE GmbH (Ltd.)*, Litzenhardtstrasse 19, Karlsruhe 76135, Karlsruhe, Germany, 2004. (c) See also <http://www.turbomole.com>. At present, TURBOMOLE is further developed and supported by COSMO logic GmbH & Co. KG, Leverkusen, Germany.
- (28) Smyth, C. P.; Rogers, H. E. *J. Am. Chem. Soc.* **1930**, *52*, 2227–2240.
- (29) Audsley, A.; Goss, F. R. *J. Chem. Soc.* **1942**, 497–500.
- (30) Harris, F. E.; Haycock, E. W.; Alder, J. J. *J. Chem. Phys.* **1953**, *21*, 1943–1948.
- (31) Riddick, J. A.; Bunger, W. B.; Sakano, T. K. *Organic Solvents. In Techniques of Chemistry*, 4th ed.; Weissberger, A., Ed.; Wiley: New York, 1986; Vol. II, p 471.

JP1009302